Electronic Supplementary Material (ESI) for Journal of Materials Chemistry C.

Supporting Information

Deciphering Intramolecular Charge Transfer in Fluoranthene Derivatives

Sanchari Debnath[1], Aisworika Mohanty[2], Praveen Naik[1], Ulrike Salzner[3], Jyotishman Dasgupta[2,*], Satish Patil[1,*]

[1]Solid State and Structural Chemistry Unit, Indian Institute of Science, Bengaluru- 560012, India.

[2]Department of Chemical Sciences, Tata Institute of Fundamental Research (TIFR), Mumbai-400005, India.

[3]Department of Chemistry, Bilkent University, Ankara 06800, Turkey.

Table of Contents:

1. General methods:

NMR Measurements: ^{1}H and ^{13}C NMR spectra were recorded on a BRUKER AVANCE-400 Fourier transformation spectrometer with 400 and 100 MHz, respectively. $CDCl_3$ and TMS were used as the solvent and internal standard, respectively. The chemical shifts are reported in parts per million (ppm) with respect to TMS. Short notations used are s for singlet, d for doublet, and t for triplet.

Mass Spectrometry Measurements: Matrix-Assisted Laser Desorption Ionization (MALDI) was performed on a Bruker daltonics Autoflex Speed MALDI-TOF System (GT0263G201) spectrometer using trans-2-[3-(4-tert-Butylphenyl)-2-methyl-2-propenylidene]malononitrile (DCTB) as the matrix.

Elemental Analysis: Elemental analyses were calculated on Thermo Scientific Flash 2000 CHNS/O Elemental Analyzer.

Thermal Measurements: Thermogravimetric analysis (TGA) was carried out using a Diamond TG/DTA instrument. The weight loss was monitored during heating from 25 to 600 °C at 2 °C min^{-1} under a nitrogen atmosphere.

Steady-state Spectroscopic Measurements: The UV-visible absorption spectra were recorded on a PerkinElmer (Lambda 35) UV-visible spectrometer. Steady-state fluorescence emission spectra were obtained using a Horiba Jobin-Yvon FluoroLog-3 spectrophotometer. Solution state UV-Vis and emission spectra were recorded in a cuvette with a path length of 1 mm.

Lifetime and Quantum Yield Measurements: Time-resolved fluorescence decay measurements were carried out with the time-correlated single photon counting (TCSPC) method with a diode laser (405 nm) in Horiba Jobin Yvon- Flurocube instrument with a pulse repetition rate of 10 MHz. The instrument response function (IRF) was collected using a scatterer (Ludox AS40 colloidal silica, Sigma-Aldrich). The quantum yield of the samples was measured by absolute method, using an integrated sphere in the Quanta-Phi instrument.

Electrochemical Measurements: CH-electrochemical analyser instrument was used to carry out cyclic voltammetry (CV) experiments. Glassy carbon was used as the working electrode,

Ag wire as the reference electrode (RE), and Platinum (Pt) wire was used as the counter electrode (CE). All experiments were carried out in anhydrous acetonitrile containing 0.1M Tetrabutylammonium hexafluorophosphate ($TBAPF_6$) as the supporting electrolyte. The reference electrode was calibrated each time before the start of experiments against Ferrocene ($E_{1/2}$ = 0.090 V vs Ag^+/Ag, $E_{1/2}$ = 0.54 V vs. SHE). All electrochemical measurements were performed at 1 mM concentration of the respective compounds. The electrolytes were purged with Ar before each experiment. The energies of the HOMO and LUMO were calculated from the onset of the oxidation and reduction potentials, respectively.

Ultrafast Transient Absorption Spectroscopic Measurements: All time-resolved measurements were done using a transient absorption spectrometer. Femtosecond laser pulses were generated in the oscillator (Coherent Micra-5 Mode-locked Ti: sapphire Laser system) with a bandwidth of ~ 90 nm at an 80 MHz repetition rate. The laser pulses were amplified in Coherent Legend Elite Ultrafast Amplifier Laser system to get ~ 30 fs/4 mJ with a repetition rate of 1 kHz and bandwidth of ~ 65 nm. For the 400 nm pump pulse, the amplifier output was directed to a BBO doubling crystal. The white-light probe continuum (420−1400 nm) was generated by focusing amplified output on a 2-mm thick sapphire, which was then directed to a multichannel detector procured from Ultrafast Systems. The pump and probe pulses were temporally and spatially overlapped within the sample. Kinetic traces have been fitted using IGOR pro 5 software with programs for deconvoluting the time constants from recorded IRF, and the singular value decomposition by Global analysis of the transient absorption data was carried out with the help of the Surface Xplorer4 and Glotaran 1.5.1 software.

Theoretical Details: The structures of **TPF**, **TPF-2Cz**, and **TPF-2TPA** were optimized without symmetry constraints with the B3P86 density functional [1] using 30% of exact exchange.[2] All calculations employ the polarized triple zeta basis sets without f-functions of Weigend et al.[3-5] Solvent effects were included with the conductor-like polarizable continuum model in cyclohexane, chloroform, and acetonitrile.[6] The first ten excited states were calculated on the ground state geometries. Then, the structures of the first excited states were optimized to obtain estimates of the Stokes shifts and emission intensities. Because some of the excited states have strong charge transfer character, the calculations on **TPF-2Cz** and **TPF-2TPA** were repeated with the long-range corrected wB97x-D3 density functional.[7] Comparison with the experiment showed that the B3P86-30% functional leads to more accurate results and was used, therefore, exclusively in the following. Excited states are characterized by natural transition orbital plots.[8] All calculations are done with the Orca program package.[9]

2. Synthetic Schemes and Procedures:

All the chemicals and reagents were purchased from Sigma-Aldrich and used without further purification. The key precursor, i.e., **DPCA** was synthesized with good yield following the previous standard reports.[10]

2.1. Synthesis of 4,4'-(ethyne-1,2-diyl) bis (N, N-diphenyl aniline) (BTPA)

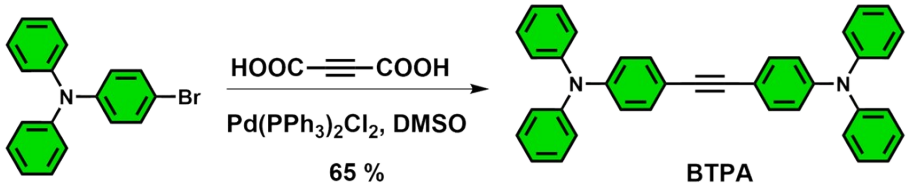

Scheme S1. Synthetic scheme for **BTPA**.

A mixture of 4-bromo triphenylamine (6.6 g, 20.34 mmol), acetylene dicarboxylic acid (1 g, 8.76 mmol), 1,4-bis(diphenylphosphino) butane (0.374 g, 0.087 mmol) and $Pd(PPh_3)_2Cl_2$ (0.3 [1]g, 0.427 mmol) in 80 mL of DMSO solution was combined with DBU (1.8 g, 17.52 mmol) and stirred at 110 °C under inert atmosphere for 3 h. After completion, the reaction mixture was allowed to reach room temperature, quenched with a saturated solution of NH_4Cl, and extracted with a DCM/water solvent mixture. Then the organic layer was evaporated under vacuum, and the resulting crude product was purified by column chromatography using silica gel (240-400 mesh) and 2-5 % ethyl acetate in hexane as eluent to obtain yellow coloured solid as the product. Yield = 65%. ^{1}H NMR (400 MHz, $CDCl_3$), δ (ppm) = 7.35 (d, 4H, J= 8 Hz), 7.28-7.27 (m, 8H), 7.12-7.10 (m, 10H), 7.06-7.03 (m, 2H), 7 (d, 4H, J= 8 Hz). The spectral data match the reported literature.[11]

2.2. Synthesis of 1,2-bis(4-(9H-carbazol-9-yl) phenyl) ethyne (BPCz)

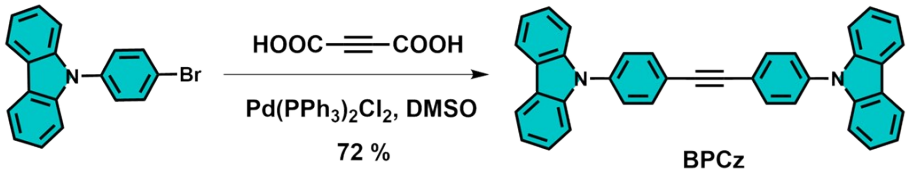

Scheme S2. Synthetic scheme for **BPCz**.

A mixture of 9-(4-bromophenyl)-9H-carbazole, acetylene dicarboxylic acid, 1,4-bis(diphenylphosphino) butane, and $Pd(PPh_3)_2Cl_2$ in DMSO solution was stirred at 110 °C under an inert atmosphere for 8 h. After completion, the reaction mixture was allowed to cool to room temperature and extracted with DCM/water. The organic layer was evaporated under vacuum, and the resulting crude product was recrystallized from methanol to get yellow coloured solid. Yield= 72 %. ^{1}H NMR (400 MHz, $CDCl_3$), δ (ppm) = 8.17-8.15 (m, 4H), 7.82 (d, 4H, J= 8 Hz), 7.62 (d, 4H, J= 8 Hz), 7.48-7.44 (m, 8H), 7.34-7.30 (m, 4H). The spectral data matches well with the reported one.[12]

2.3. General method for synthesis of phenylene-based fluoranthene derivatives.

A mixture of 7,9-diphenyl-8H-cyclopenta[a]acenaphthylen-8-one (**DPCA**) and respective acetylene derivatives *i.e.,* ethynylbenzene (for **TPF**), 1,2-bis(4-(9H-carbazol-9-yl) phenyl) ethyne (for **TPF-2Cz**) and 4,4'-(ethyne-1,2-diyl) bis (N, N-diphenyl aniline) (for **TPF-2TPA**) in 15 mL of 4-nitrobenzene was taken in hydrothermal bomb and was kept in furnace at 220 °C for 72 h. Once the reaction was over, the reaction mixture was diluted with water, followed by extraction with CH_2Cl_2 (30 mL × 3). The solvent was removed under reduced pressure. The resulting crude was treated with activated charcoal and recrystallized with DCM/methanol to get the desired phenylene-based fluoranthene derivatives with a high yield.

7,8,10-triphenylfluoranthene-TPF

Greenish-yellow solid (yield= 90 %). ^{1}H NMR (400 MHz, $CDCl_3$), δ (ppm) = 7.75-7.70 (m, 4H), 7.57-7.50 (m, 3H), 7.39-7.36 (m, 6H), 7.33 (s, 1H), 7.30 (d, 2H, J= 6 Hz), 7.24-7.22 (m, 2H), 7.19-7.16 (m, 3H), 6.69 (d, 1H, J= 4 Hz); ^{13}C NMR (100 MHz, $CDCl_3$), δ (ppm): 141.07, 140.84, 139.39, 138.29, 137.99, 136.68, 136.25, 135.98, 135.77, 133.20, 131.24, 130.40, 130.04, 129.78, 129.21, 128.72, 128.55, 127.90, 127.72, 127.63, 127.37, 126.73, 126.43, 123.43, 123.01. MS (MALDI-TOF): calculated for $C_{34}H_{22}$: 430.172, found: 430.042 $[M]^{+\cdot}$. The spectral data matches well with the reported literature.[10]

9,9'-((7,10-diphenylfluoranthene-8,9-diyl)bis(4,1-phenylene))bis(9H-carbazole)-TPF-2Cz

White solid (yield = 86 %). ^{1}H NMR (400 MHz, $CDCl_3$), δ (ppm) = 8.09 (t, 4H, J= 4 Hz), 7.78 (d, 2H, J= 4 Hz), 7.46-7.41 (m, 10H), 7.37 (t, 2H, J= 6 Hz), 7.23-7.18 (m, 16H), 7.08 (t, 4H, J= 4 Hz), 6.82 (d, 2H, J= 8 Hz); ^{13}C NMR (100 MHz, $CDCl_3$), δ (ppm) = 140.89, 139.92, 139.60, 139.57, 137.37, 137.02, 136.32, 135.05, 133.41, 132.93, 130.32, 129.79, 128.52, 127.83, 127.34, 126.93, 126, 125.81, 123.56, 123.24, 120.26, 119.78, 109.56. MS (MALDI-TOF): calculated for $C_{64}H_{40}N_2$: 837.038, found: 837.378 $[M]^{+\cdot}$.

4,4'-(7,10-diphenylfluoranthene-8,9-diyl)bis(N,N-diphenylaniline)-TPF-2TPA

Pale yellow solid (yield= 85 %). ^{1}H NMR (400 MHz, $CDCl_3$), δ (ppm) = 7.72 (d, 2H, J= 4 Hz), 7.36-7.33 (m, 10H), 7.29 (t, 2H, J= 6 Hz), 7.16 (t, 8H, J= 6 Hz), 6.92 (t, 4H, J= 6 Hz), 6.87 (d, 8H, J= 4 Hz), 6.79 (d, 4H, J= 4 Hz), 6.73-6.68 (m, 6H). ^{13}C NMR (100 MHz, $CDCl_3$), δ (ppm) = 147.88, 145.08, 140.61, 139.96, 137.38, 136.56, 136.43, 135.24, 133.33, 132.41, 130.33, 129.71, 129.11, 128.21, 127.71, 126.90, 126.58, 123.62, 123.28, 123.23, 122.23. MS (MALDI-TOF): calculated for $C_{64}H_{44}N_2$: 841.070, found: 841.339 $[M]^{+\cdot}$.

3. Characterization Spectra:

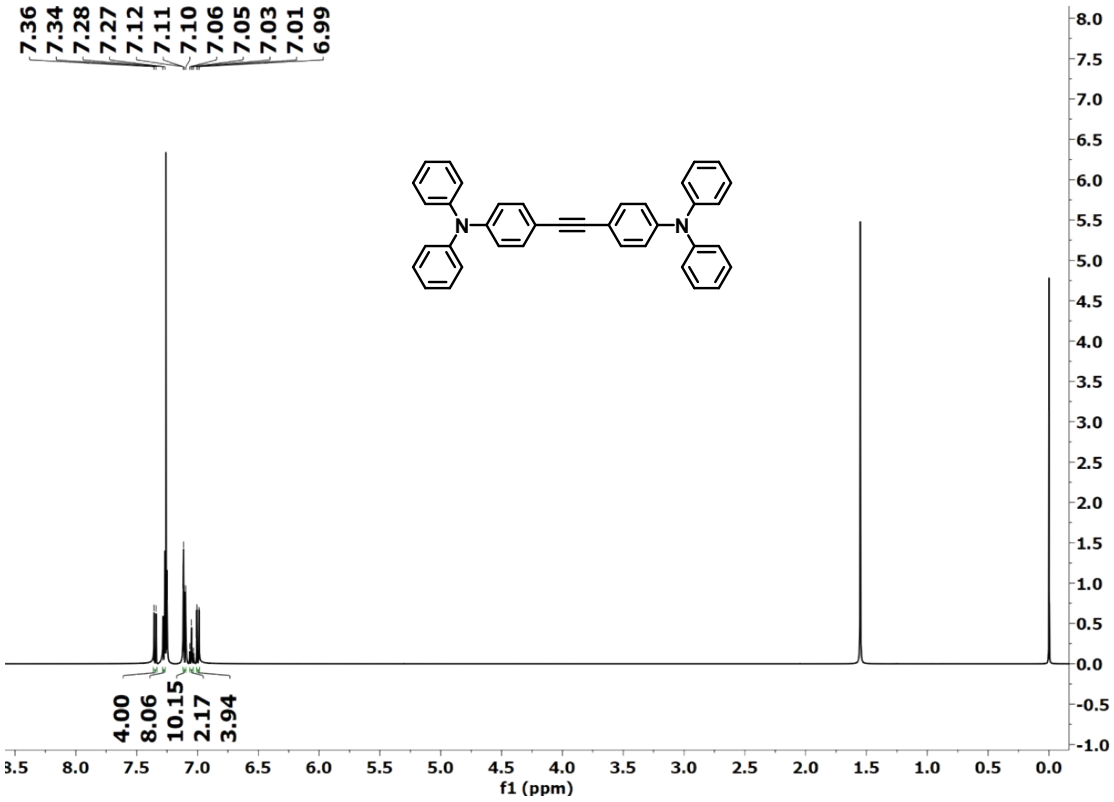

Figure S1. ^{1}H NMR spectrum of **BTPA** in $CDCl_3$.

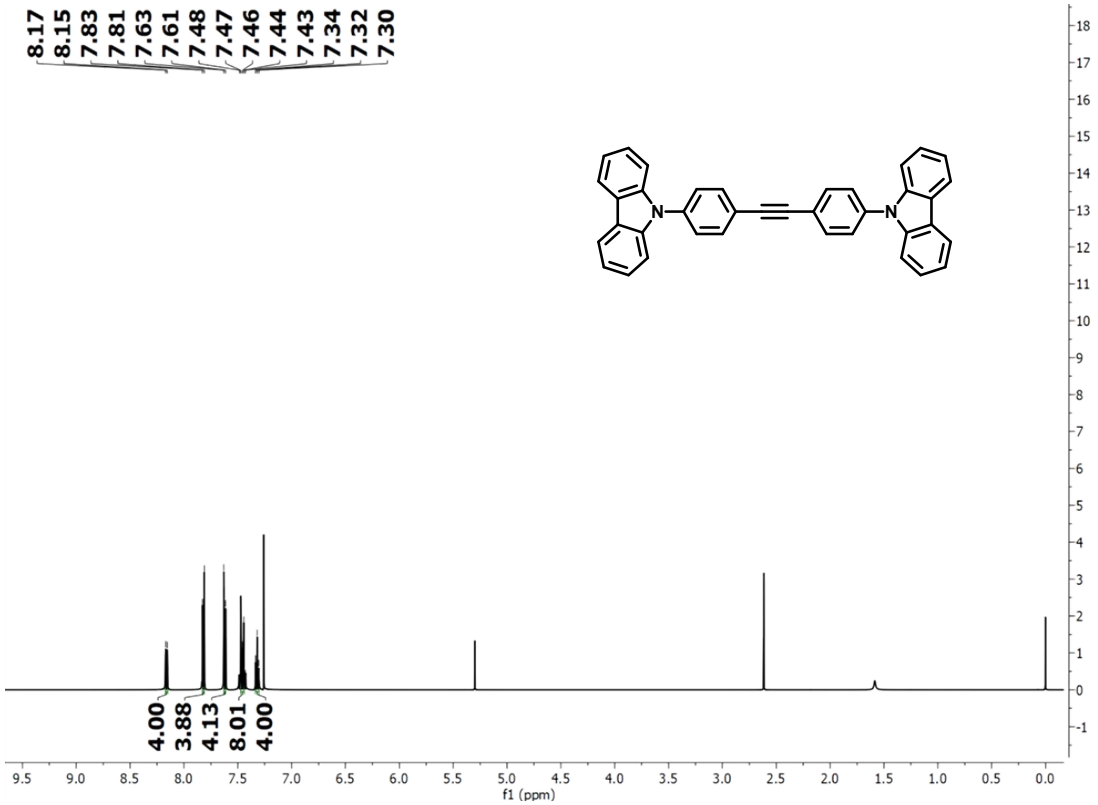

Figure S2. ^{1}H NMR spectrum of **BPCz** in $CDCl_3$.

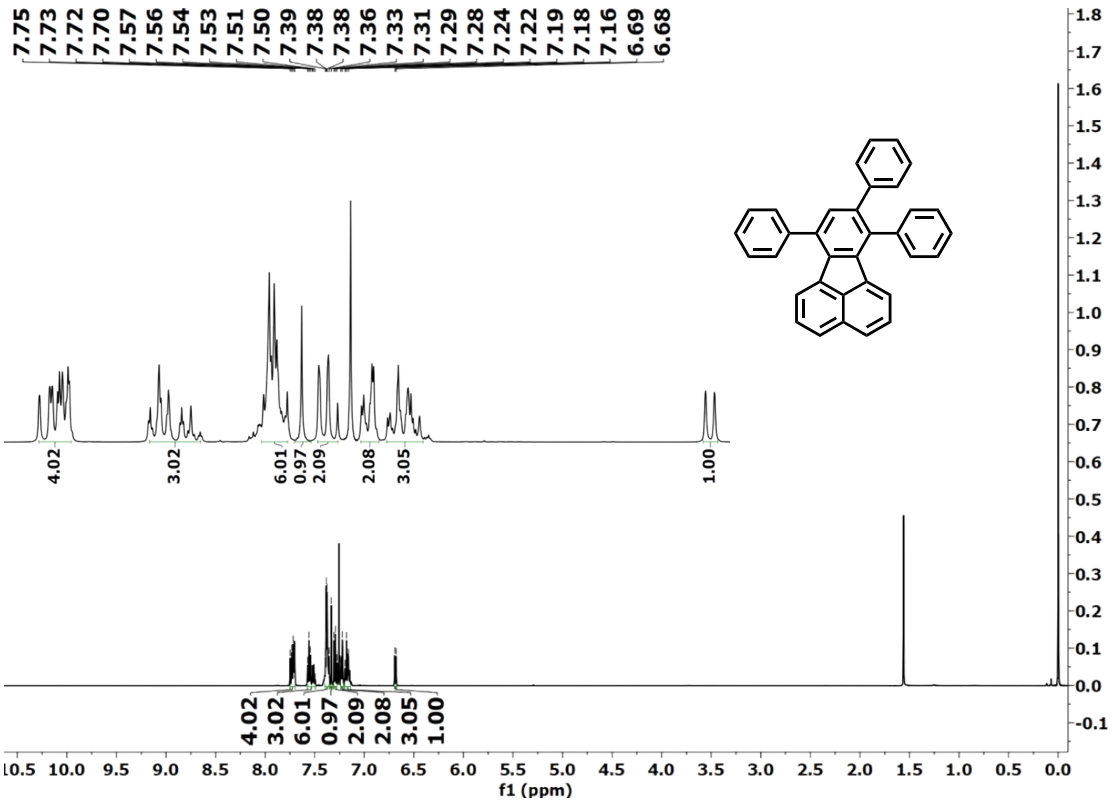

Figure S3. ^{1}H NMR spectrum of **TPF** in $CDCl_3$.

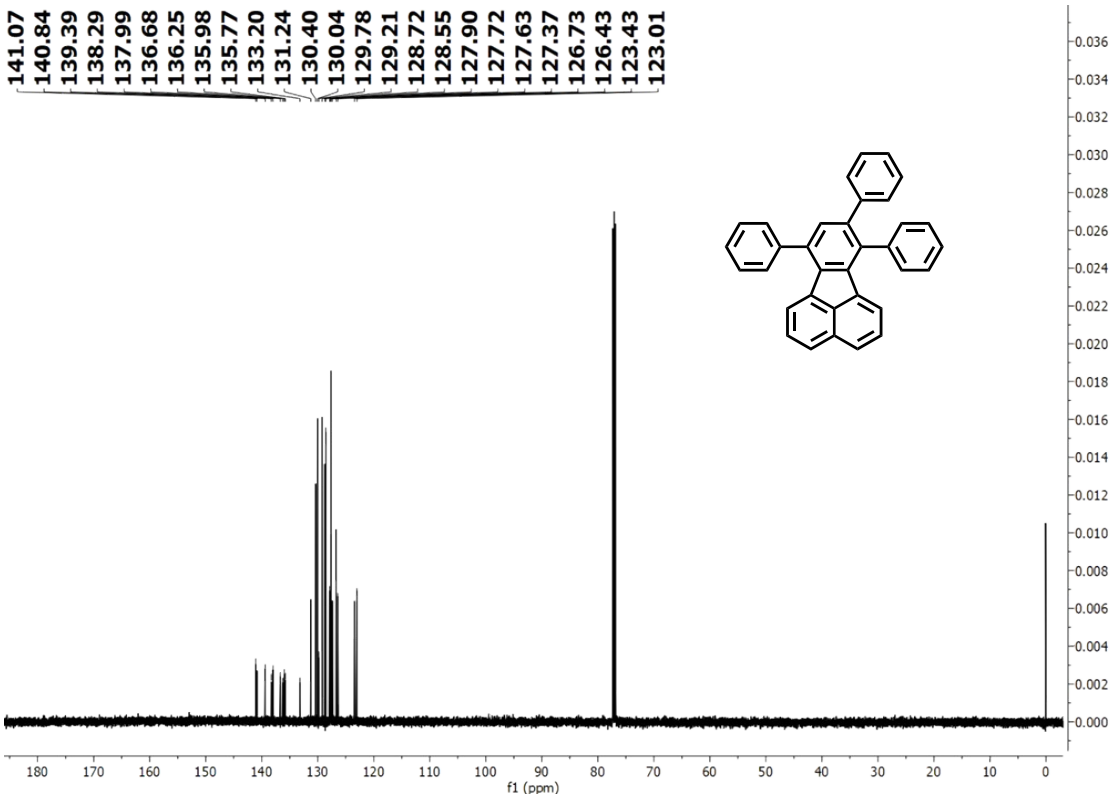

Figure S4. ^{13}C NMR spectrum of **TPF** in $CDCl_3$.

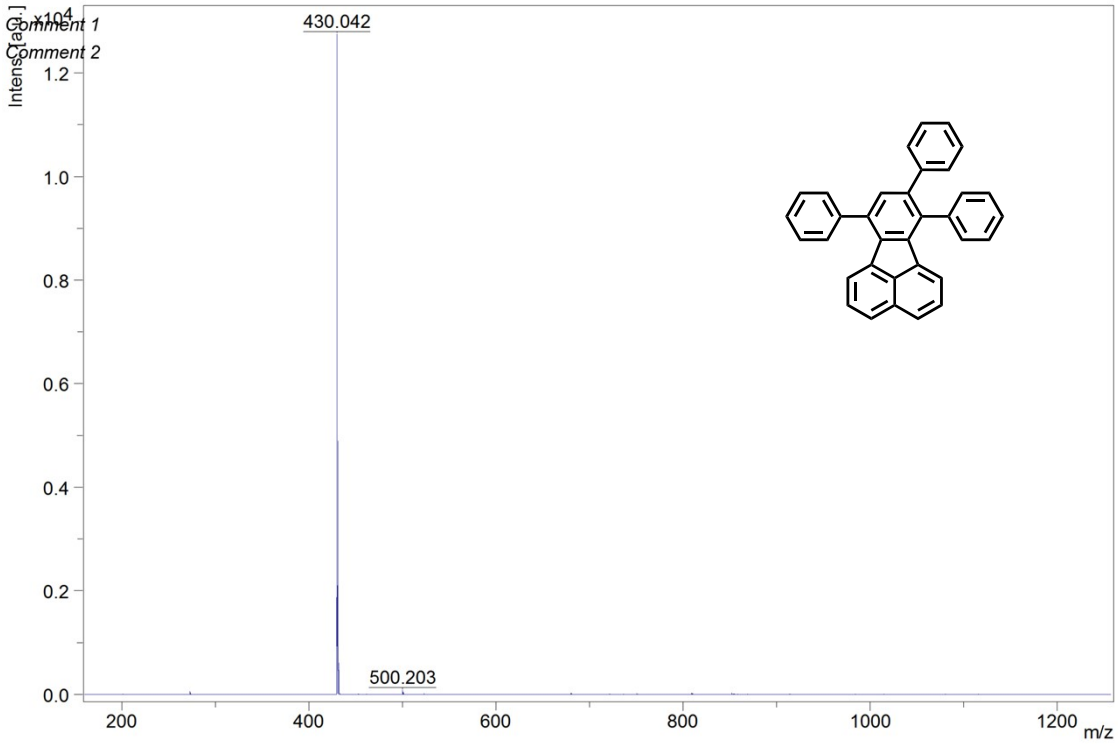

Figure S5. MALDI spectrum of **TPF**.

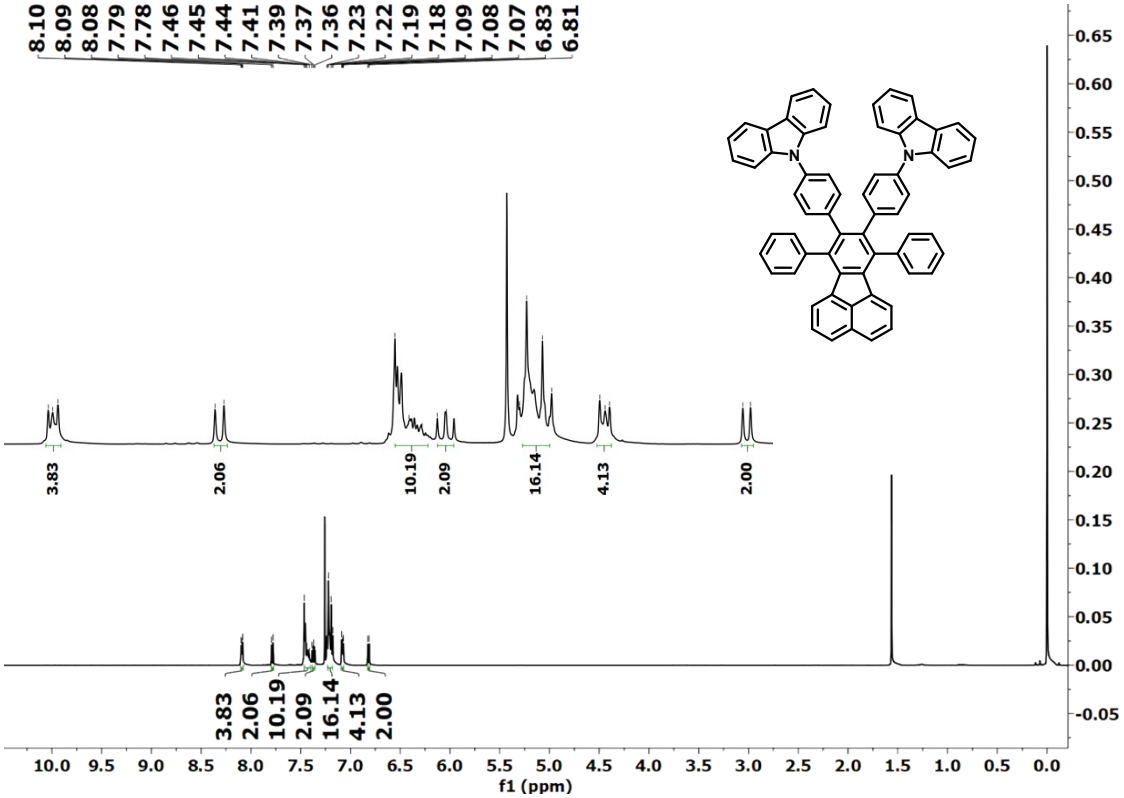

Figure S6. ^{1}H NMR spectrum of **TPF-2Cz** in $CDCl_3$.

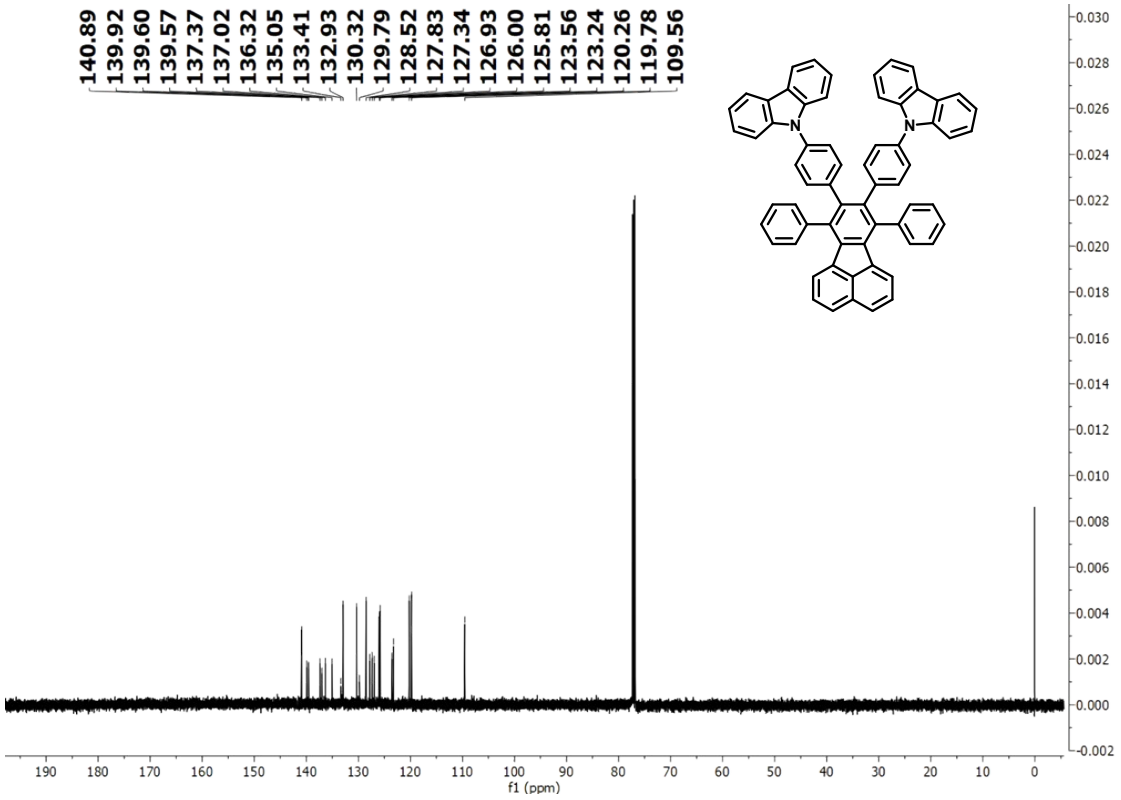

Figure S7. ^{13}C NMR spectrum of **TPF-2Cz** in $CDCl_3$.

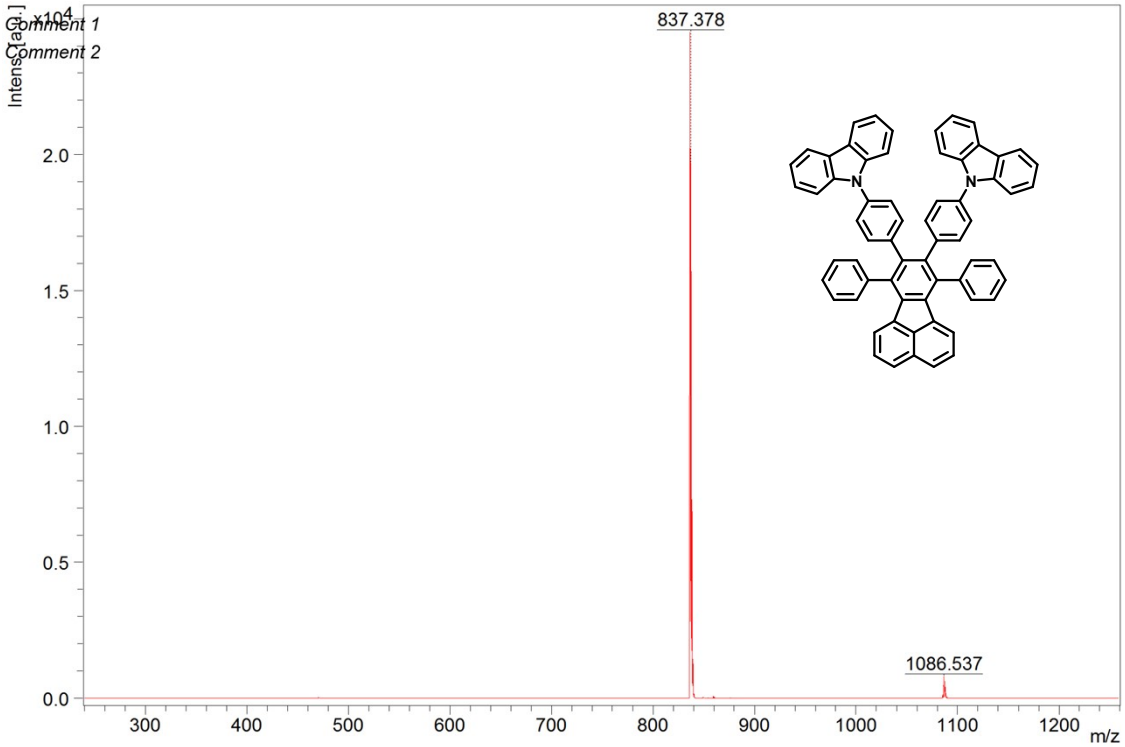

Figure S8. MALDI spectrum of **TPF-2Cz**.

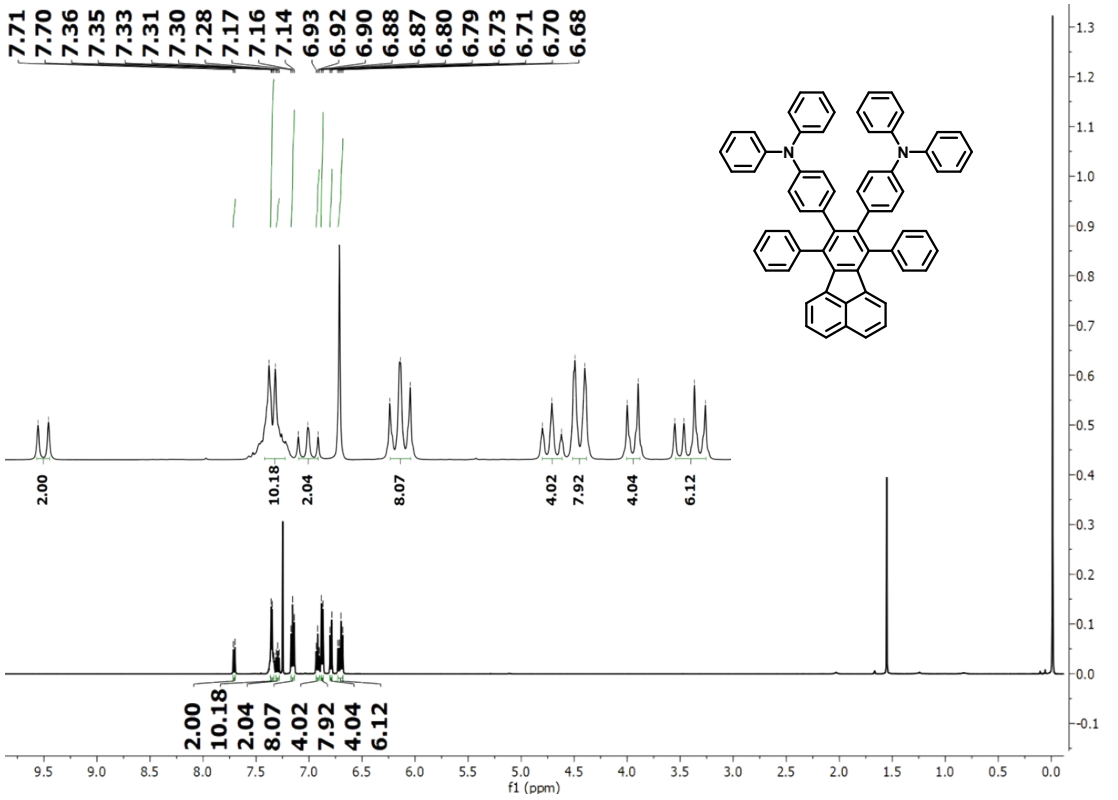

Figure S9. ^{1}H NMR spectrum of **TPF-2TPA** in $CDCl_3$.

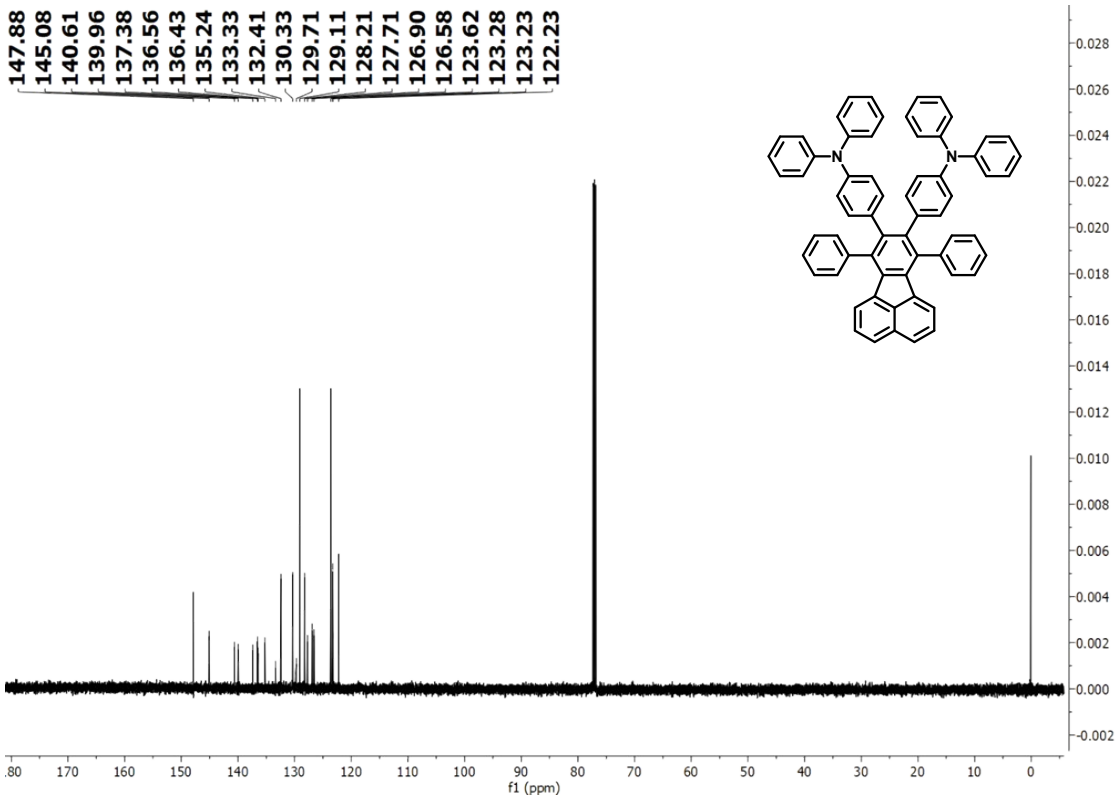

Figure S10. ^{13}C NMR spectra of **TPF-2TPA** in $CDCl_3$.

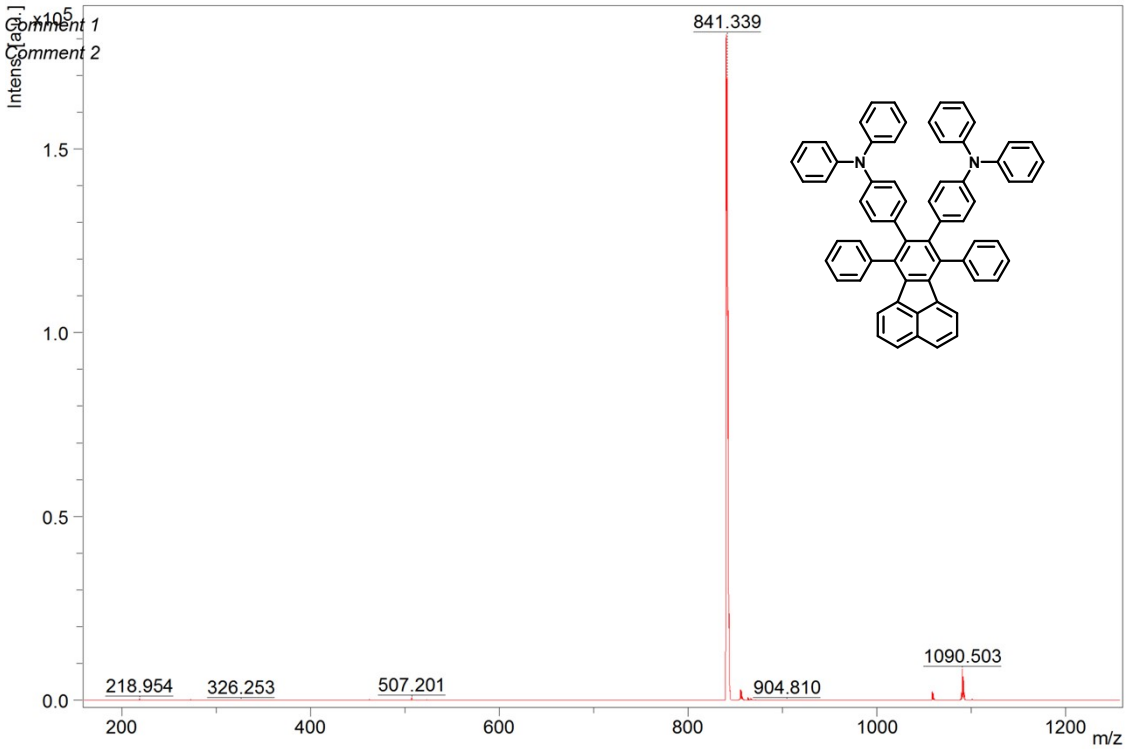

Figure S11. MALDI spectrum of **TPF-2TPA**.

4. Supporting Figures:

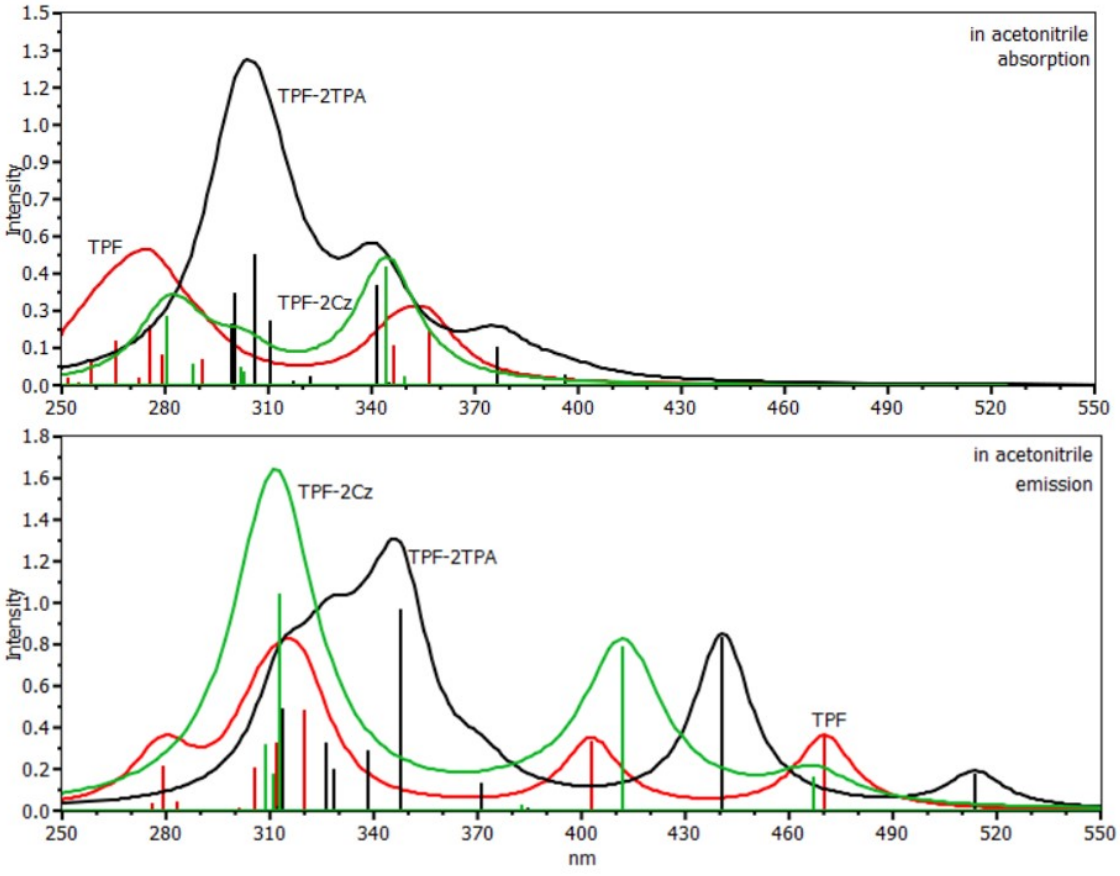

Figure S12. Simulated UV-visible absorption spectra in ACN using optimized S_0 structures (top) and 'emission' spectra (bottom) based on optimized S_1 structures of three fluoranthene derivatives calculated using B3P86-30 %/TVP-f level of theory.

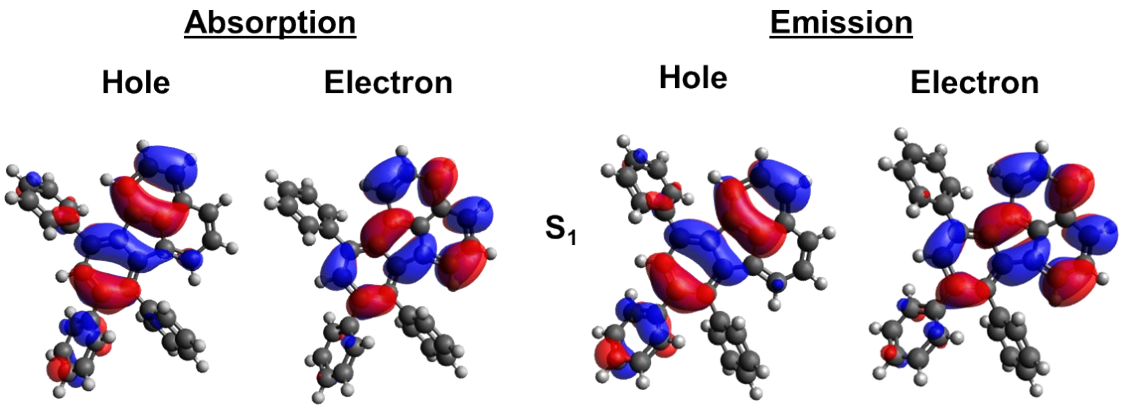

Figure S13. Natural transition orbitals (NTOs) for transition between ground state (S_0) and first excited state (S_1) of **TPF** in acetonitrile (calculated using B3P86-30 %/TVP-f level of theory).

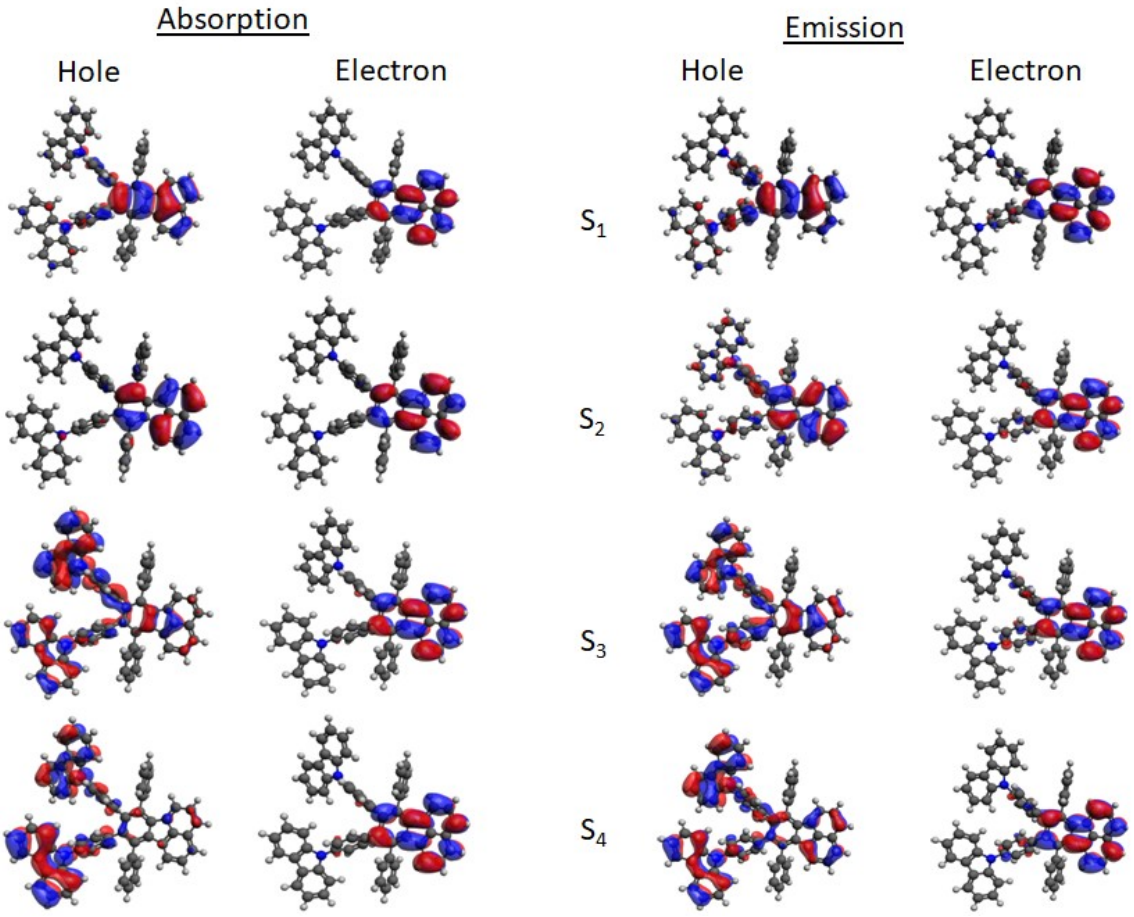

Figure S14. Natural transition orbitals (NTOs) for transition between ground state (S_0) and first four excited states (S_1 through S_4) of **TPF-2Cz** in acetonitrile (calculated using B3P86-30 %/TVP-f level of theory).

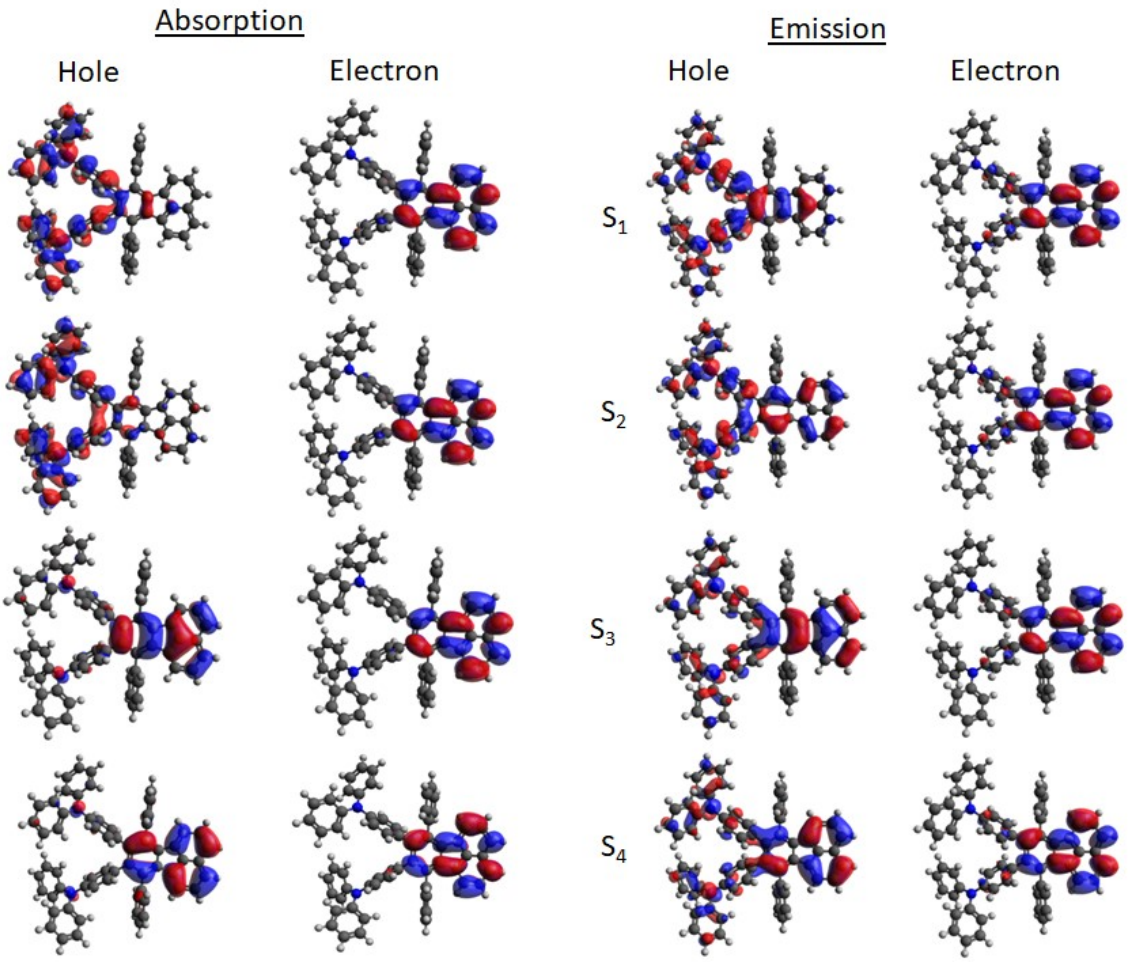

Figure S15. Natural transition orbitals (NTOs) for transition between ground state (S_0) and first four excited states (S_1, through S_4) of **TPF-2TPA** in acetonitrile (calculated using B3P86-30 %/TVP-f level of theory).

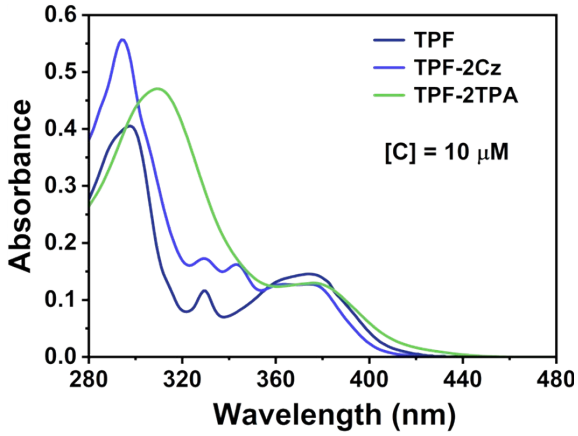

Figure S16. UV-visible absorption spectra of **TPF**, **TPF-2Cz,** and **TPF-2TPA** in solution ([C]= 10 μM, and chloroform was used as a solvent in all cases).

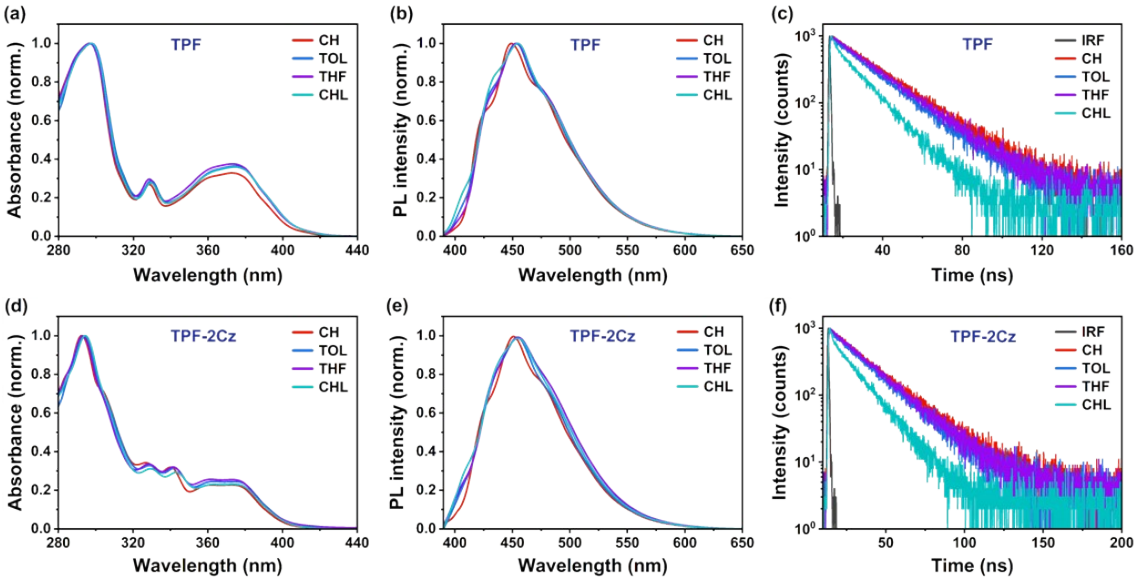

Figure S17. (a), (d) Normalized UV-visible absorption, (b), (e) normalized PL spectra, and (c), (f) time-resolved decay plots of **TPF** and **TPF-2Cz,** respectively, in different solvents upon increasing the solvent polarity ([c] = 10 μM, $\lambda_{exc.}$ = 380 nm; For TCSPC measurement, $\lambda_{exc.}$ = 405 nm, $\lambda_{collected}$ = 455 nm for CH, TOL, THF, CHL, and ACN in **TPF**; $\lambda_{collected}$ = 450, 455, 455, 455, and 460 nm, respectively, for the solvents CH, TOL, THF, CHL, and ACN, in **TPF-2Cz**). (All the time-resolved decay plots were fitted using mono-exponential decay function)

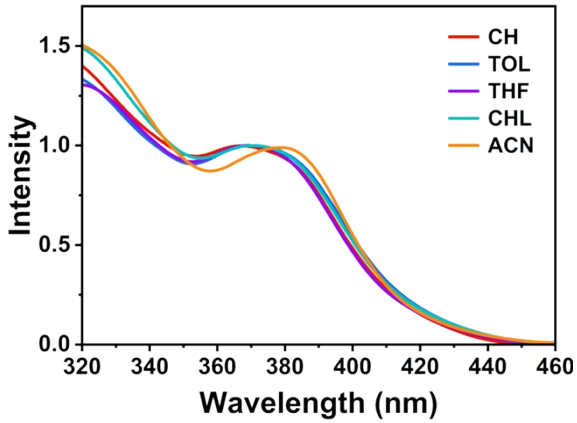

Figure S18. Normalized excitation spectra of **TPF-2TPA** in different solvents upon increasing the solvent polarity ([c] = 10 μM, excitation spectra were collected at the respective emission maxima).

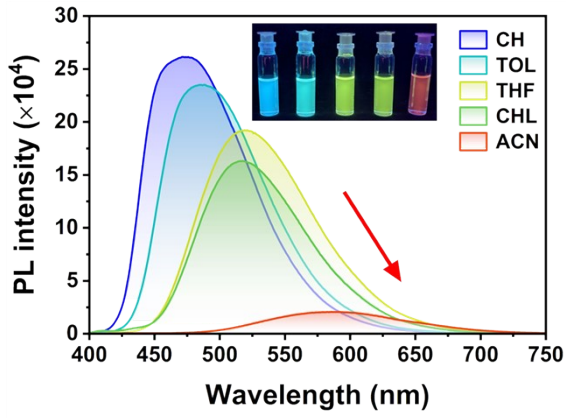

Figure S19. PL emission spectra of **TPF-2TPA** in solvents of different polarities ([c] = 10 μM, $\lambda_{exc.}$ = 380 nm. The inset photograph was taken under UV light at 365 nm excitation, showing the emission behaviour in different solvents).

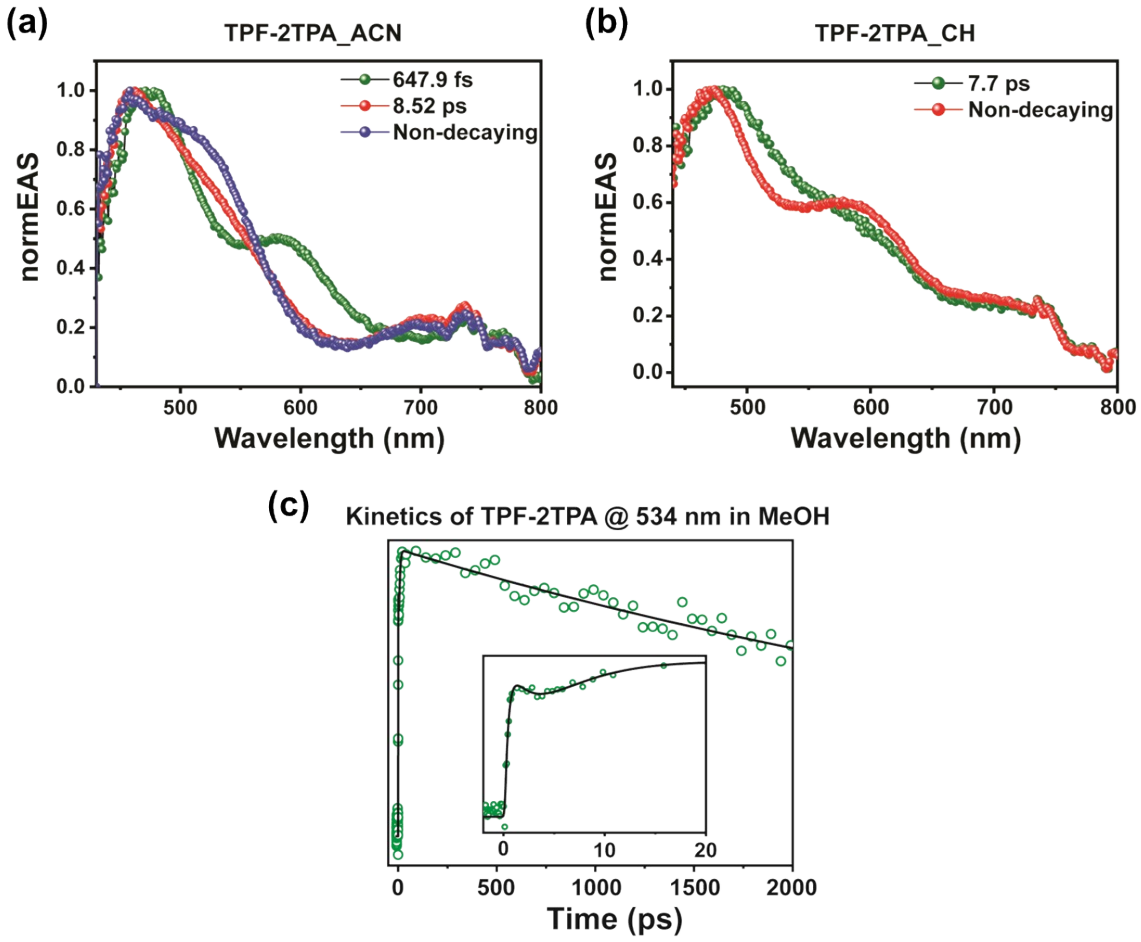

Figure S20. Two-state sequential singular value decomposition of the TA spectra of 100 μM **TPF-2TPA** in (a) Acetonitrile and (b) Cyclohexane. (c) Single point kinetic fitting of **TPF-2TPA** @ 534 nm in methanol.

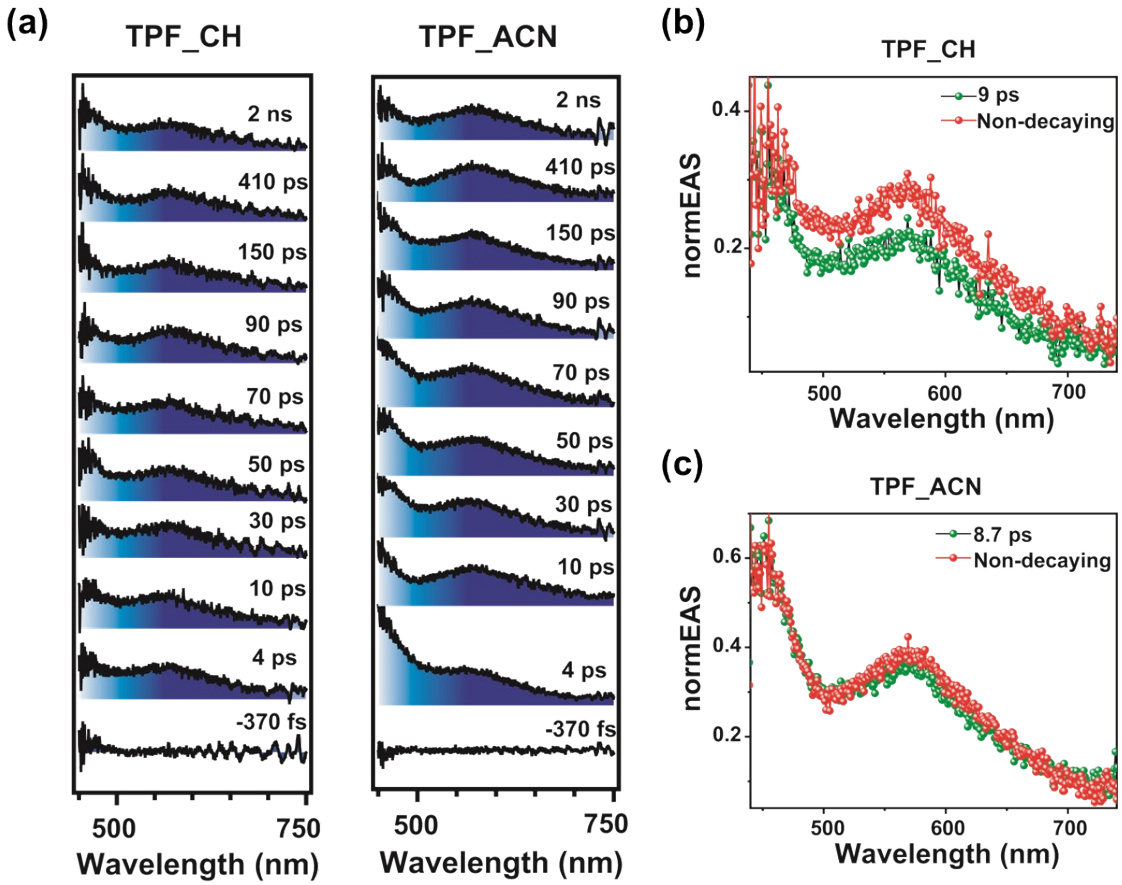

Figure S21. (a) Transient Absorption spectra of **TPF** in different solvents upon photoexcitation at 400 nm. Two-state sequential singular value decomposition of the TA spectra of **TPF** in (b) cyclohexane (CH) and (c) acetonitrile (ACN).

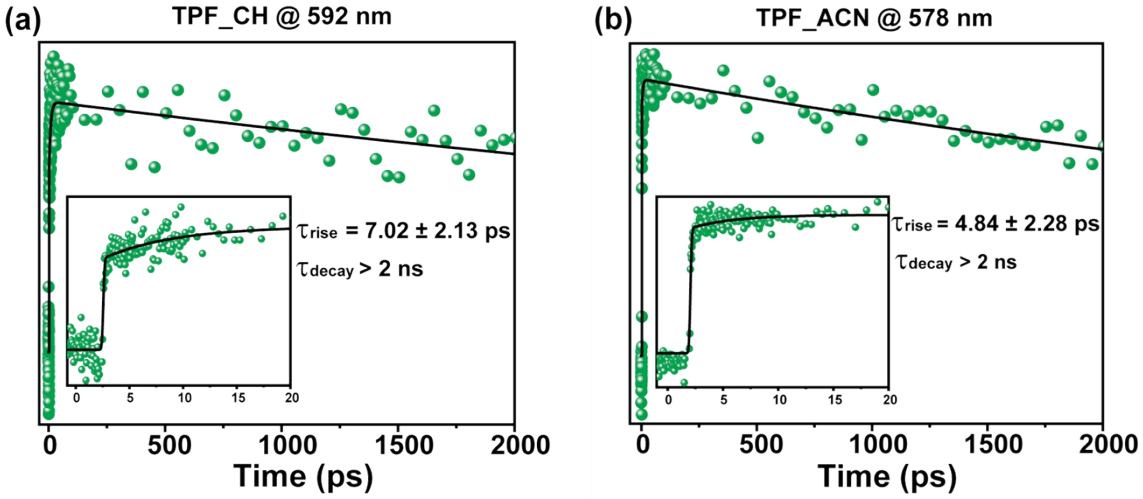

Figure S22. Single point kinetic fitting of **TPF** in (a) cyclohexane @ 592 nm and (b) acetonitrile @ 578 nm.

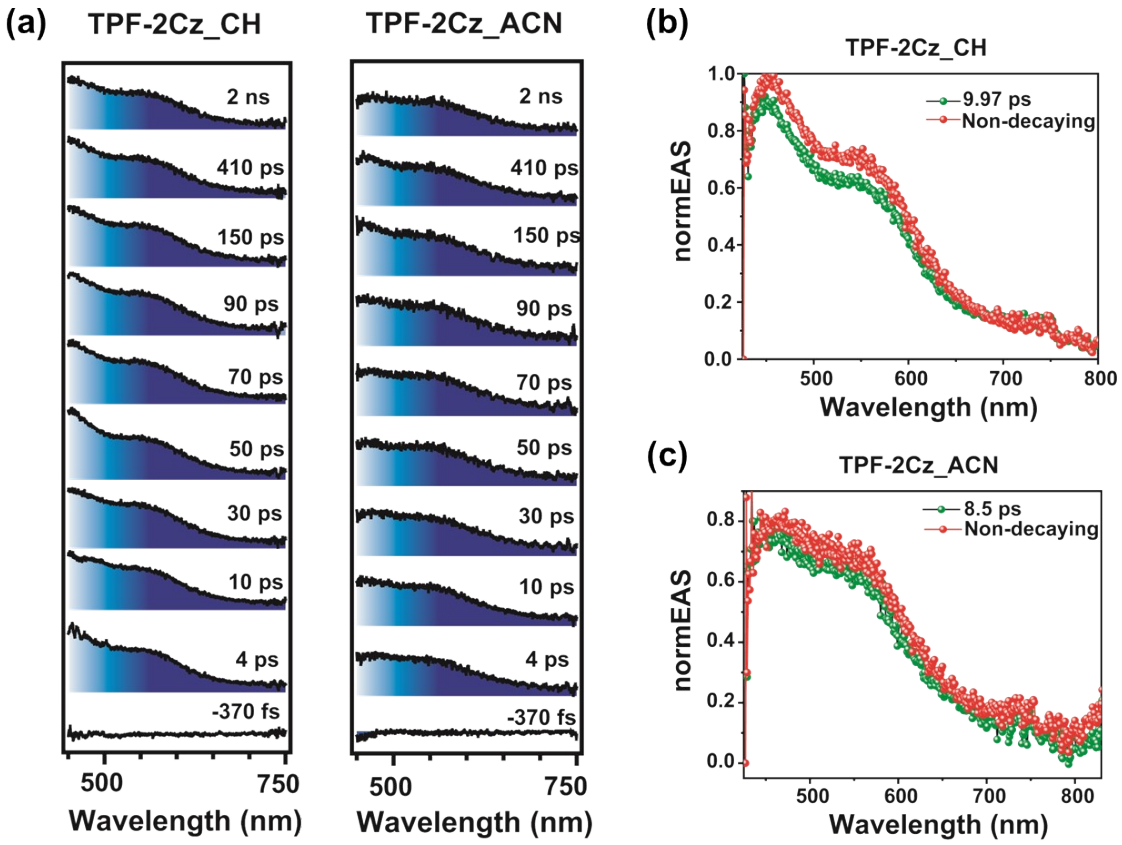

Figure S23. (a) Transient Absorption spectra of **TPF-2Cz** in different solvents upon photoexcitation at 400 nm. Two-state sequential singular value decomposition of the TA spectra of **TPF-2Cz** in (b) Cyclohexane (CH) and (c) Acetonitrile (ACN).

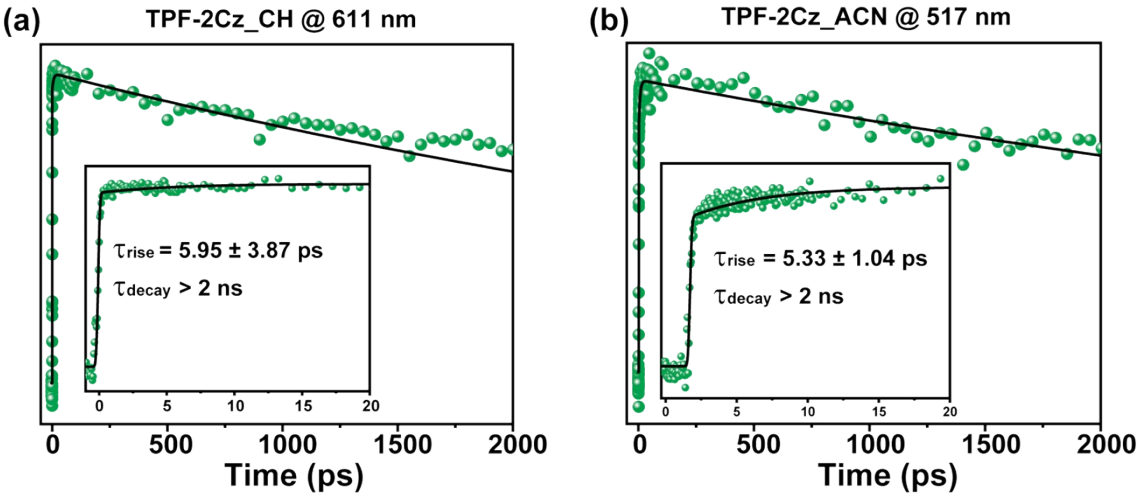

Figure S24. Single point kinetic fitting of **TPF-2Cz** in (a) cyclohexane @ 611 nm and (b) acetonitrile @ 517 nm.

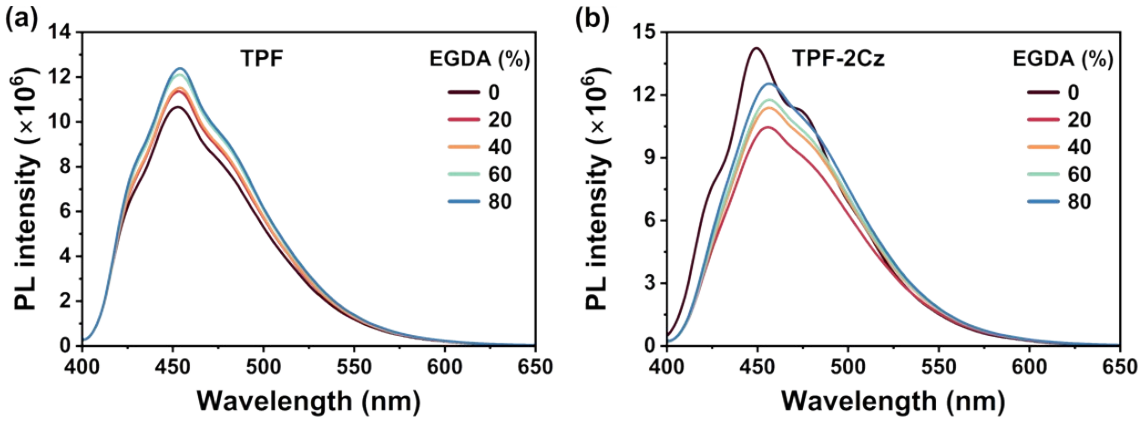

Figure S25. Changes in the PL emission spectra of (a) **TPF** and (b) **TPF-2Cz** upon increase in the ethylene glycol diacetate (EGDA) fraction in methanol. ([c] = 10 μM, $\lambda_{exc.}$ = 380 nm for PL experiment)

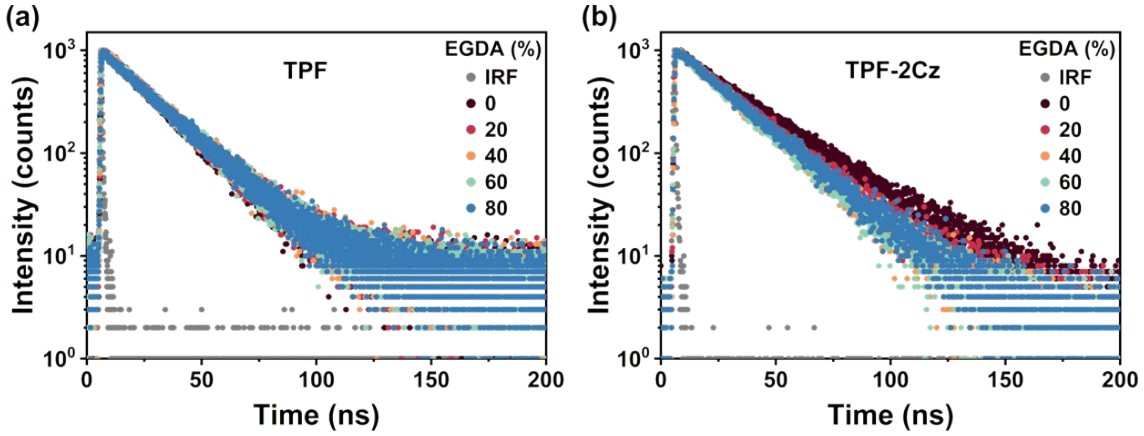

Figure S26. Time-resolved emission decays of (a) **TPF** and (b) **TPF-2Cz** in different ethylene glycol diacetate (EGDA)-methanol mixtures. ($\lambda_{exc.}$ = 405 nm and collected at respective emission maxima, IRF= Instrument Response Function, All the time-resolved decay plots were fitted using mono-exponential decay function)

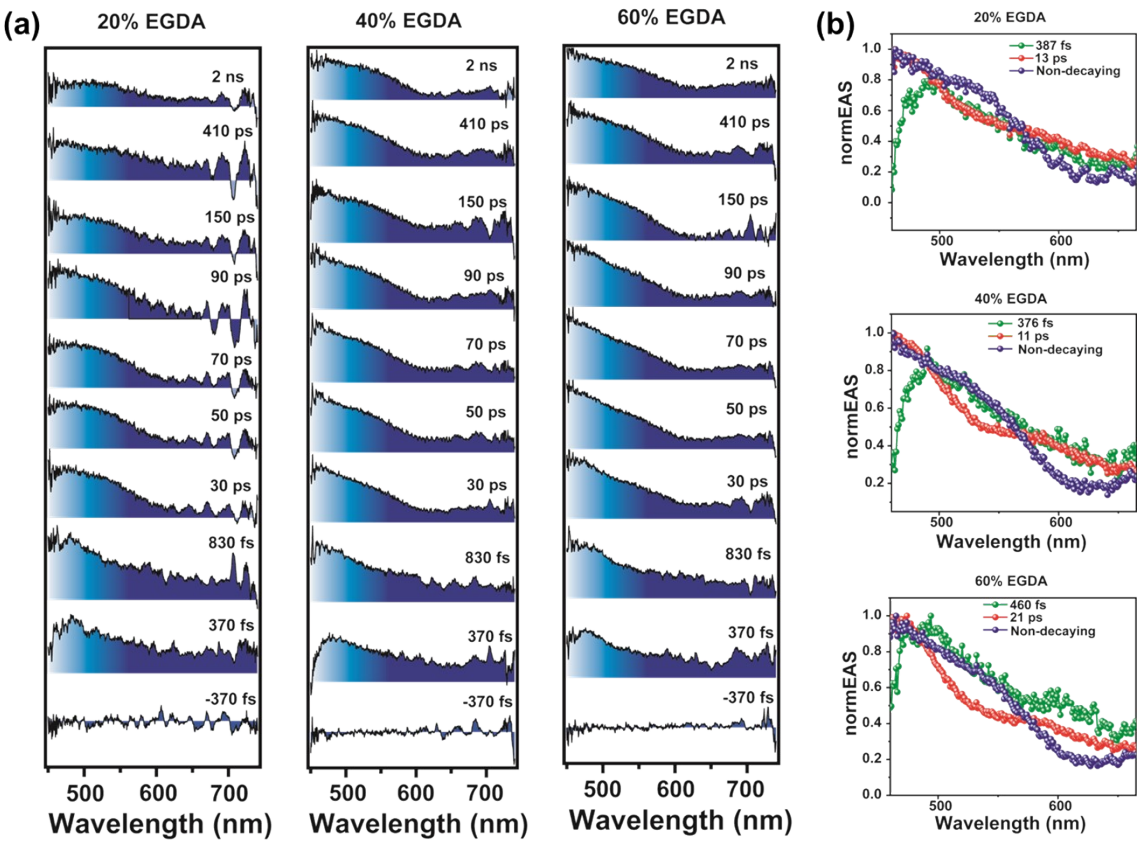

Figure S27. (a) Transient Absorption spectra of 100 μM **TPF-2TPA** with varying ethylene glycol diacetate (EGDA) percentage in methanol upon photoexcitation at 400 nm. (b) Three-state sequential singular value decomposition (SVD) of the TA spectra of **TPF-2TPA** with varying ethylene glycol percentage upon photoexcitation at 400 nm.

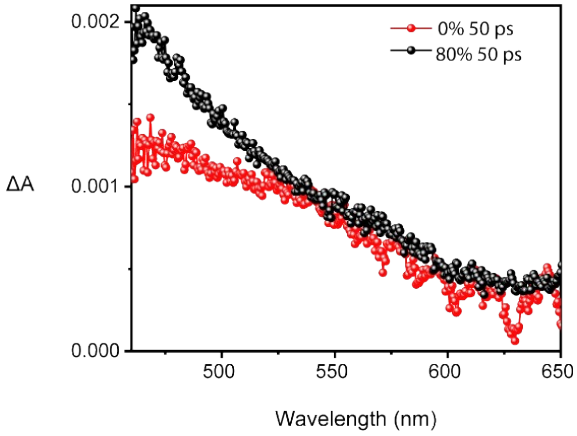

Figure S28. Comparison of Transient Absorption (TA) spectra of 100 μM **TPF-2TPA** at 50 ps in 0 and 80% EGDA in methanol upon photoexcitation at 400 nm.

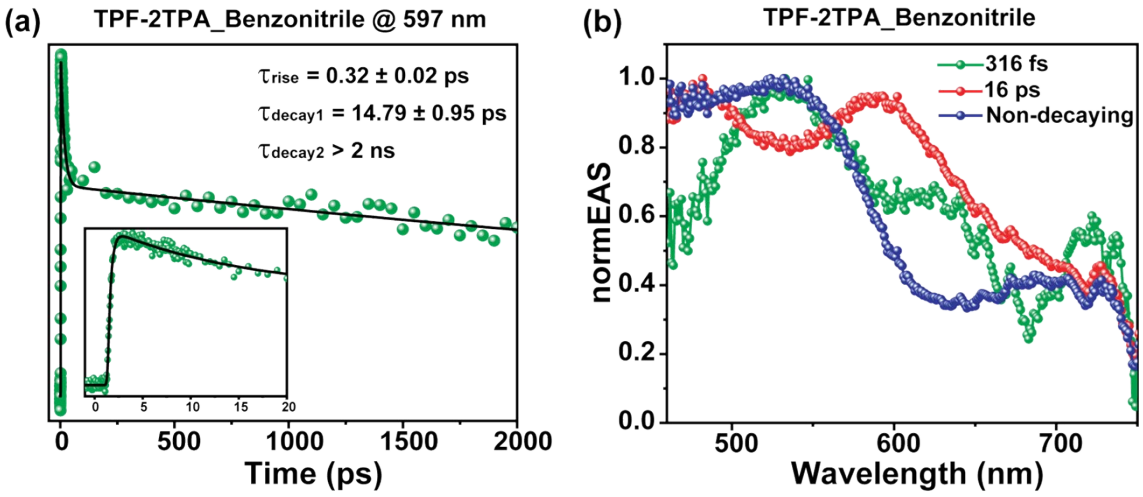

Figure S29. (a) Single point kinetic fitting of **TPF-2TPA** @ 597 nm in benzonitrile and (b) Two-state sequential singular value decomposition of the TA spectra of 100 μM **TPF-2TPA** in benzonitrile.

5. Supporting Tables:

Table S1. Predicted vertical transitions for **TPF** and their assignments (calculated using B3P86-30 %/TVP-f level of theory in acetonitrile).

Compound	$\lambda_{abs.}$ (nm)	f	Assignment	
TPF	357	0.21	HOMO→ LUMO	66 %
			HOMO-1→ LUMO	28 %
	347	0.16	HOMO-1→ LUMO	65 %
			HOMO→ LUMO	29 %
	291	0.1	HOMO-4→ LUMO	39 %
			HOMO→ LUMO+1	24 %
			HOMO-2→ LUMO	8 %
	279	0.12	HOMO-2→ LUMO	51 %
			HOMO-3→ LUMO	19 %
			HOMO-1→ LUMO+1	13 %
	276	0.24	HOMO→ LUMO+1	36 %
			HOMO-2→ LUMO	32 %
			HOMO-1→ LUMO+1	14 %
			HOMO-3→ LUMO	10 %

Table S2. Predicted vertical transitions for **TPF-2Cz** and their assignments (calculated using B3P86-30 %/TVP-f level of theory in acetonitrile).

Compound	$\lambda_{abs.}$ (nm)	f	Assignment	
	349.8	0.03	HOMO-5→ LUMO	75 %
			HOMO→ LUMO	19 %
	344.3	0.47	HOMO-2→ LUMO	85 %
			HOMO-1→ LUMO	10 %
	334.4	0.001	HOMO→LUMO	78 %
			HOMO-5→ LUMO	17 %
	328	0.004	HOMO-1→ LUMO	87 %
			HOMO-2→ LUMO	10 %
	303.2	0.05	HOMO→ LUMO+1	47 %

TPF-2Cz			HOMO-1→ LUMO+1	23 %
			HOMO→ LUMO+2	14 %
			HOMO-1→ LUMO+1	10 %
	302.3	0.07	HOMO-1→ LUMO+1	33 %
			HOMO→ LUMO+2	32 %
			HOMO-1→ LUMO+3	20 %
	293.7	0.00	HOMO-3→ LUMO	100 %
	292.2	0.00	HOMO-3→ LUMO	100 %
	288.3	0.08	HOMO-8→ LUMO	52 %
			HOMO-2→ LUMO+5	11 %
	280.8	0.28	HOMO→ LUMO+2	62 %

Table S3. Predicted vertical transitions for **TPF-2TPA** and their assignments (calculated using B3P86-30 %/TVP-f level of theory in acetonitrile).

Compound	**$\lambda_{abs.}$ (nm)**	**f**	**Assignment**	
TPF-2TPA	396	0.04	HOMO→ LUMO	95 %
	377	0.15	HOMO−1→ LUMO	95 %
	345	0.01	HOMO−3→ LUMO	90 %
	342	0.40	HOMO−2→ LUMO	91 %
	322	0.04	HOMO→ LUMO+1	53 %
			HOMO−1→ LUMO+4	14 %
			HOMO→ LUMO+2	12 %

Table S4. Summary of the experimental S_1 energies for **TPF-2TPA** in solvents of different polarities (S_1 energies are calculated from the high energy onsets of the PL emission spectra).

Solvent	**λ_{onset} (nm)**	**E_{S1} (eV)**
Cyclohexane	425	2.92
Toluene	436	2.84
Tetrahydrofuran	452	2.74
Chloroform	452	2.74
Acetonitrile	491	2.52

Table S5. Fluorescence lifetimes of **TPF-2TPA** upon an increase in viscosity of the medium (EGDA in methanol was used; [c] = 10 μM, $\lambda_{exc.}$ = 380 nm for PL, for TCSPC measurement, $\lambda_{exc.}$ = 405 nm). (All the time-resolved decay plots were fitted using mono-exponential decay function).

EGDA (%)	**$\lambda_{em.}$ (nm)**	**τ (ns)**	**χ^2**
0	555	4.02	1.06
10	549	5.12	1.10
20	547	6.35	1.16
30	545	7.86	1.16
40	543	9.20	1.13
50	542	10.64	1.20
60	538	11.87	1.08
70	537	12.89	1.18

80	532	13.72	1.16
90	530	14.11	1.12

Table S6. Fluorescence lifetimes of **TPF** upon an increase in viscosity of the medium (EGDA in methanol was used; [c] = 10 μM, $\lambda_{exc.}$ = 380 nm for PL, for TCSPC measurement, $\lambda_{exc.}$ = 405 nm) (All the time-resolved decay plots were fitted using mono-exponential decay function).

EGDA (%)	τ (ns)	χ^2
0	19.74	1.16
20	20.32	1.21
40	20.44	1.16
60	20.73	1.14
80	20.91	1.20

Table S7. Fluorescence lifetimes of **TPF-2Cz** upon an increase in viscosity of the medium (EGDA in methanol was used; [c] = 10 μM, $\lambda_{exc.}$ = 380 nm for PL, for TCSPC measurement, $\lambda_{exc.}$ = 405 nm). (All the time-resolved decay plots were fitted using mono-exponential decay function).

EGDA (%)	τ (ns)	χ^2
0	28.53	1.05
20	23.93	0.99
40	22.10	1.00
60	21.94	1.06
80	22.87	1.04

6. References:

[1] A. D. Becke, *J. Chem. Phys.,* 1993, **98**, 5648–5652.

[2] U. Salzner, P. Pickup, R. Poirier and J. Lagowski, *J. Phys. Chem. A*, 1998, **102**, 2572–2578.

[3] F. Weigend, *Phys. Chem. Chem. Phys.*, 2006, **8**, 1057–1065.

[4] F. Weigend and R. Ahlrichs, *Phys. Chem. Chem. Phys.*, 2005, **7**, 3297–3305.

[5] A. Hellweg, C. Hättig, S. Höfener and W. Klopper, *Theor. Chem. Acc.*, 2007, **117**, 587–597.

[6] V. Barone and M. Cossi, *J. Phys. Chem. A*, 1998, **102**, 1995–2001.

[7] Y. Lin, G. Li, S. Mao and J. Chai, *J. Chem. Theory Comput.*, 2013, **9**, 263–272.

[8] R. L. Martin, *J. Chem. Phys.*, 2003, **118**, 4775–4777.

[9] F. Neese, *Wiley Interdiscip. Rev.: Comput. Mol. Sci.*, 2022, **12**, e1606.

[10] S. Kumar, D. Kumar, Y. Patil and S. Patil, *J. Mater. Chem. C*, 2016, **4**, 193–200.

[11] Z. Zhuang, F. Bu, W. Luo, H. Peng, S. Chen, R. Hu, A. Qin, Z. Zhao and B. Z. S. Tang, *J. Mater. Chem. C*, 2017, **5**, 1836–1842.

[12] R. Furue, T. Nishimoto, I. S. Park, J. Lee and T. Yasuda, *Angew. Chem., Int. Ed.*, 2016, **55**, 7171–7175.